Songklanakarin J. Sci. Technol.
43 (6), 1701-1707, Nov. - Dec. 2021

http://www.sjst.psu.ac.th

Original Article

Determination of water content of a residual soil slope in response to infiltrating rainwater using transient seepage model and its verification♣

Thitinan Indhanu[1], Panupong Thumtuan[2], Tanan Chub-Uppakarn[2], and Tanit Chalermyanont[2*]

[1] *Southern Natural Disaster Research Center, Prince of Songkla University, Hat Yai, Songkhla, 90110 Thailand*

[2] *Department of Civil Engineering, Faculty of Engineering, Prince of Songkla University, Hat Yai, Songkhla, 90110 Thailand*

Received: 18 December 2020; Revised: 16 March 2021; Accepted: 7 May 2021

Abstract

Reduction of soil shear strength is significant in evaluating slope failure for rainfall-induced landslide study. Increasing soil water content due to infiltrating rainwater increases pore water pressure and decreases the shear strength of soil. In this paper, transient seepage simulations were conducted to determine the change of pore water pressure and water content of the soil in a test pit in response to rainfall. Simulation results were verified by comparing to field monitoring data recorded from time domain reflectometers installed in the test pit. Simulation results showed that the topsoil solely responded to the rain as its pore water pressure promptly changed from negative to positive indicating that the infiltrating rainwater had changed the soil from unsaturated to saturated soil. For deeper soils, due to their low permeability, their pore water pressures slightly increased as the water in the topsoil marginally flowed downward but it mostly drained downslope to slope toe. The simulated volumetric water content compared fairly well to the observed one as percent errors were lower than 10 percent.

Keywords: transient seepage model, residual soil slope, volumetric water content, pore water pressure

1. Introduction

Rainfall-induced landslides in residual soil slopes are common in tropical regions around the world (Brunetti, Peruccacci, Rossi, Luciani, Valigi, & Guzzetti, 2010; Jiratananuvong, Chalermyanont, & Chub-Uppakarn, 2016; Matsushi & Matsukura, 2007; Montgomery, Dietrich, Torres, Anderson, Heffner, & Loague, 1997; Rahardjo, Leong, & Rezaur, 2002; Uchida, Asano, Ohte, & Mizuyama, 2003; Wolle & Hachich, 1989). Residual soil slopes are naturally shallow and unsaturated. Infiltration of rainwater of a wetting front leads to development of perched water table resulting in an increase in pore water pressure or reduction in soil matric suction which, in turn, results in decreasing in the shear strength of the soil, reducing the stability of the soil slope, and ultimately triggering the slope failure (Ng & Shi, 1998; Rezaur, Rahardjo, Leong, & Lee, 2003).

Slope instability can be assessed when reduction of the soil shear strength is known using the water content that increased due to infiltration of rainwater. Increase in the water content can be measured in-situ using installed instrumentations. Rahardjo *et al.* (2002) and Rezaur *et al.* (2003) used tensiometers to determine the hydrological response of the residual soil slopes in Singapore. The tensiometers were used to measure positive and negative pore water pressure of saturated and unsaturated soils. Also, the water content can be measured using a time domain reflectometer (TDR). As described in Quinones, Ruelle, & Nemeth (2003) and Topp, Davis, & Annan (1980) measurement of the soil moisture content using the TDR is made via a soil dielectric constant.

♣Peer-reviewed paper selected from The 9th International Conference on Engineering and Technology (ICET-2021)
*Corresponding author
Email address: tanit.c@psu.ac.th

Alternatively, hydrological models have been applied to predict the soil water content (Acharya, Bhandary, Dahal, & Yatabe, 2016; Frattini, Crosta, & Sosio, 2009; Iverson 2000). The models simulate the water movement in both unsaturated and saturated soils while soil hydraulic conductivity is no longer a constant value in the unsaturated soil and it is defined by soil-water content hydraulic conductivity function (Anderson & Pope 1984; Leach & Herbert 1982). The water movement is used to describe the change in pore water pressure using groundwater flow governing equation (Ng & Shi 1998). The pore water pressure is converted to soil water content using water pressure-water content relationships, so-called a soil-water characteristic curve (SWCC).

Evaluation of real-time stability of the soil slope subjected to rainfall can be assessed using coupled hydrological-slope stability models such as SEEP/W and SLOPE/W (GeoStudios 2012, GEO-SLOPE International, Ltd.) with the time series data of the soil water content obtained from the hydrological models. Chalermyanont & Chup-uppakarn (2020) developed a pilot real-time landslide warning system which real-time measurement of rainfall and soil water content along with the computed real time slope stability (i.e., factor of safety) were displayed publicly on the website. The study showed that real time determination of landslide is possible for a particular soil slope where proper hydrological and geotechnical properties are available.

The objectives of this paper are to determine the soil water contents due to infiltration of rainwater using the hydrological model and to verify them by comparing with the field measured data obtained from the TDRs. For this purpose, a selected site in Songkhla province, southern Thailand was studied. Hydrological and geotechnical properties of the soil slope at the site were determined. A hydrological model was developed and the soil water contents were simulated. The TDRs were installed in the slope and real-time variations of soil water content with depth were measured.

2. Study Area

The study area (Figure 1) is located at the hillslope at the Faculty of Engineering, Prince of Songkla University, which is a part of the Kho Hong Mountain, Hat Yai City, Songkhla Province, in Southern Thailand. Geologically, the parent rocks here are carboniferous sandstone, shale and conglomerate, while the residual soil is mainly lateritic soils (Department of Mineral Resources, 2007). The height and slope angle of the slope is about 5 m and 24 degrees, respectively. The residual soil is relatively thin with a thickness of about 2-3 m. Underneath the residual soil is the weathered rock.

3. Physical and Hydrological Soil Properties

A test pit of 1 m in diameter and 2.2 m deep was dug to collect soil samples for determination of physical and hydrological properties of the residual soil and to perform water content monitoring using TDRs (Figure 2). Disturbed and undisturbed soil samples were collected for a series of laboratory tests. The soil samples were analyzed for physical properties such as Atterberg's limits, particle size, and soil classification and other hydrological and engineering properties according to the ASTM standards.

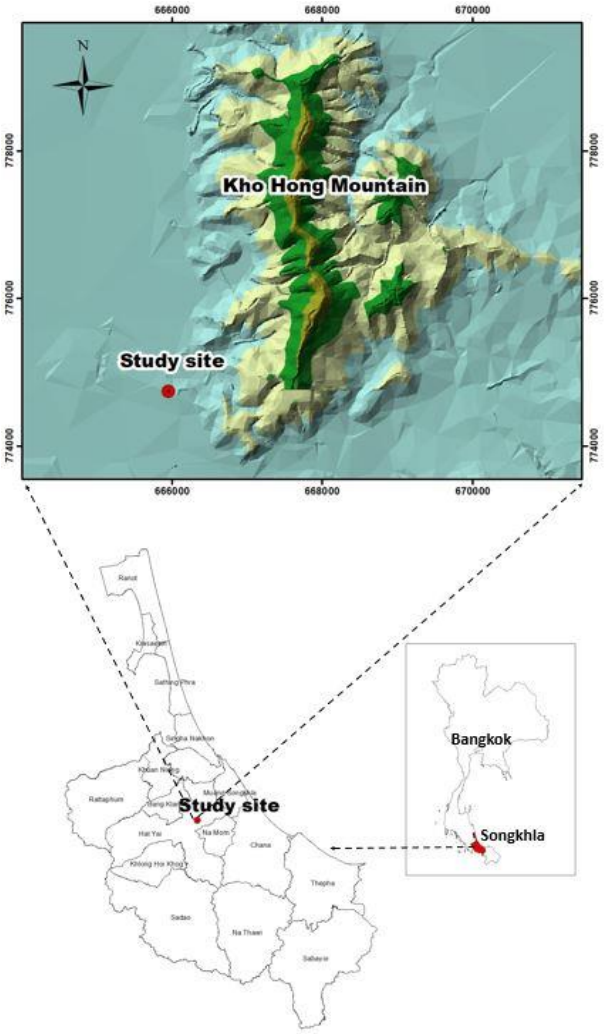

Figure 1. Maps showing location of the study area

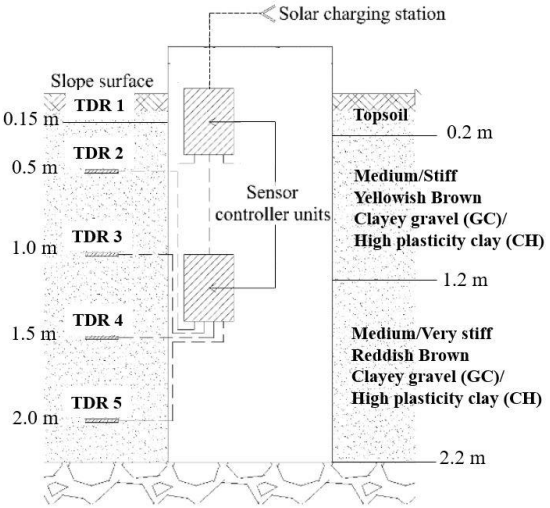

Figure 2. Cross section of the test pit

3.1 Physical properties and soil profile

Physical properties of the soils are shown in Table 1 and described in authors' previous works (Chalermyanont & Chup-uppakarn, 2020; Thumtuan, Chup-Uppakarn, & Chalermyanont, 2018). A soil profile of the slope is shown in Figure 2. The residual soil consists of three layers. The topsoil layer with organic substance and vegetation, classified as silty sand (SM), is about 0.2 m thick. The upper soil layer, classified as clayey gravel (GC) or high plasticity clay (CH), is 1.0 m thick. Lastly, the lower soil layer with thickness of 1.0 m is also classified as GC or CH but it differs from the upper layer by its color and strength.

3.2 Hydraulic conductivity tests

For the topsoil, an infiltration test was performed on the ground surface to determine hydraulic conductivity of the soil using a double-ring infiltrometer (ASTM D 3385). Test result shows that hydraulic conductivity of the topsoil is 2.30×10^{-3} cm/s. For the deeper soils, a set of the falling head tests (ASTM 5084) was conducted on undisturbed samples collected from the test pit at the depth of 0.5 and 1.5 m. The test results show that the hydraulic conductivities are 3.80×10^{-7} cm/s and 4.30×10^{-7} cm/s for the upper and lower soils, respectively.

3.3 Kunzelstab penetration test

Kunzelstab penetration test (DIN 4094-2002) is a light-weight cone penetration test that provides a measure of penetration resistance which can be used to determine the shear strength of soils. Kunzelstab penetration resistance (N_{KPT}) of the soils in the test pit was obtained by conducting the tests for every 20 cm interval. The N_{KPT} obtained was subsequently converted to the standard penetration resistance (N_{SPT}) using an empirical equation proposed by EGAT (1980). The N_{KPT} and N_{SPT} are tabulated in Table 1 and indicate that the lower soil (N_{SPT} = 21 blows/ft) is denser or stiffer than the upper one (N_{SPT} = 12 blows/ft).

4. Transient Seepage Model

To determine the change of soil water content during the rainfall that affects the soil strength and the stability of the soil slope, SEEP/W and SLOPE/W programs have been widely used (Acharya *et al.* 2016; Lee, Gofar, & Rahardjo, 2009; Rahardjo, Ong, Rezaur, & Leong, 2007; Rahimi, Rahardjo, & Leong, 2010;). In this study, the SEEP/W which is a finite element-based program was used to simulate transient seepage of water in soil slope. It uses a numerical discretization technique to solve Darcy's equations for unsaturated and saturated flow conditions and runs a water-flow governing equation (Equation 1) in each time step to compute two-dimensional seepage (Fredlund & Rahardjo, 1993).

$$\frac{\partial}{\partial x}\left(k_x \frac{\partial H}{\partial x}\right) + \frac{\partial}{\partial y}\left(k_y \frac{\partial H}{\partial y}\right) + q = m_w^2 \gamma_w \frac{\partial H}{\partial t} \quad (1)$$

where k_x is the hydraulic conductivity in x-direction; k_y is the hydraulic conductivity in y-direction; H is the hydraulic head or total head; q is the applied flux at the boundary; m_w is the slope of soil-water characteristic curve; and γ_w is the unit weight of water.

4.1 Finite element mesh and boundary conditions

In this study, a two-dimensional transient seepage finite element modeling of the slope was conducted. The finite element mesh is shown in Figure 3. The slope domain was discretized into a series of 0.1 m-quadrilateral elements with a total of 9,728 nodes and 3,129 elements. To simulate natural flow, appropriate boundary conditions were assigned to the boundaries of the slope. Rainfall boundary was assigned to the slope surface (i.e., line A-B-C-D). No flow boundary was assigned to the left boundary (line A-H) to prevent seepage contribution from upper slope sections. No flow boundary was also assigned to the bottom boundary (line E-F-G-H) to practically simulate the impervious layer of weathered rock underneath the lower soil layer. For the right boundary (line

Table 1. Soil properties of the study slope

Properties	Topsoil (0 - 0.2 m)	Upper soil (0.2 - 1.2 m)	Lower soil (1.2 - 2.2 m)
Physical			
Gravel (%)	12.35	36.54 - 45.65	34.26 - 42.52
Sand (%)	65.36	15.53 - 22.63	9.17 - 10.54
Fines (%)	22.29	38.82 - 40.83	45.90 - 55.91
Bulk density (kN/m^3)	17.4	18.1 - 20.3	18.6 - 21.6
Water content (%)	13.99	10.73 - 15.11	13.72 - 18.68
Saturated volumetric water content	0.35	0.32	0.33
Liquid limit (%)	34.87	38.45 - 42.58	49.71 - 52.81
Plastic limit (%)	24.63	18.84 - 21.11	25.61 - 29.55
Plasticity index (%)	10.24	19.61 - 21.47	23.26 - 24.10
Specific gravity	2.67	2.72 - 2.77	2.72 - 2.76
USCS classification	SM	GC, CH	GC, CH
Hydrological			
Hydraulic conductivity (cm/sec)	2.30×10^{-3}	3.80×10^{-7}	4.30×10^{-7}
Penetration Resistance			
N_{KPT} (blows/20 cm)	10	22	38
N_{SPT} (blows/ft)	6	12	21
Relative density / Consistency	Loose	Medium / stiff	Medium / very stiff

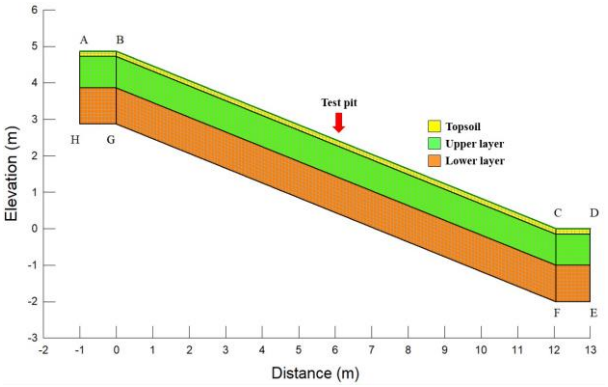

Figure 3. Finite element model of the soil slope

D-E), a unit gradient boundary was assigned to allow free drainage out of the slope domain. Initial groundwater table was not known but it was practically set to be located at 3 m below the ground surface in order to match the simulation results to the measured data.

4.2 Rainfall data

Time series rainfall data from October 15th to November 30th, 2016 were used as model input (Figure 4). For wetting period (October 15th to November 5th, 2016), there were many storms, where the maximum daily rainfall was 60.2 mm on October 26th and the cumulative rainfall was 308 mm. After November 6th, very little rainfall was recorded, thus, from this day on till the end of simulation. This period is referred to as "drying period". Time discretization in the simulation (time step) was set to be an hour per time step. Thus, a total of 1,080 time steps were simulated.

4.3 Soil water characteristic curve and hydraulic conductivity function

In transient seepage modeling of an unsaturated soil, the soil water characteristic curve (SWCC) and the hydraulic conductivity function (HCF) are significant input. The SWCC is a relationship between soil volumetric water content and matric suction (i.e., negative pore water pressure). The volumetric water content is defined by the ratio of water volume to soil volume. In this study, the SWCCs for three soil layers were estimated from GeoStudio (2012) for similar soil types. The SWCCs obtained, then, were validated by comparing with corresponding SWCCs acquired from the Unsaturated Soil Type Database (UNSODA) (Nemes, Schaap, Leij, & Wösten, 2001). For the HCF, it describes a relationship between soil hydraulic conductivity and matric suction. The HCFs used in this study were estimated from the SWCCs just obtained using Fredlund & Xing (1994) criterion. The SWCCs and HCFs used in the modeling are shown in Figure 5.

4.4 In-situ water content monitoring

To verify the seepage simulation results, volumetric water content was used. It was measured in-situ using the TDRs. Topp *et al.* (1980) stated that a TDR is employed to determine soil moisture content via a dielectric constant of the

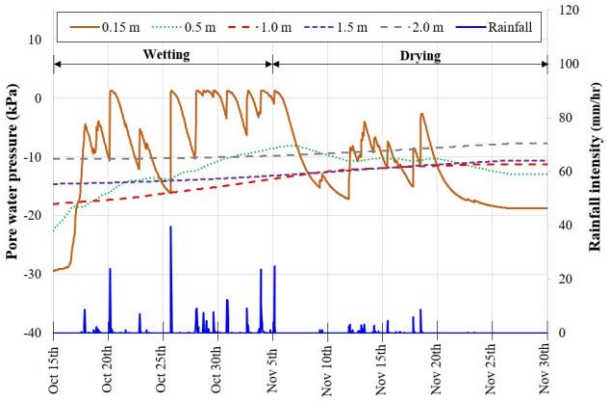

Figure 4. Time series of rainfall data and simulated pore water pressure at the test pit

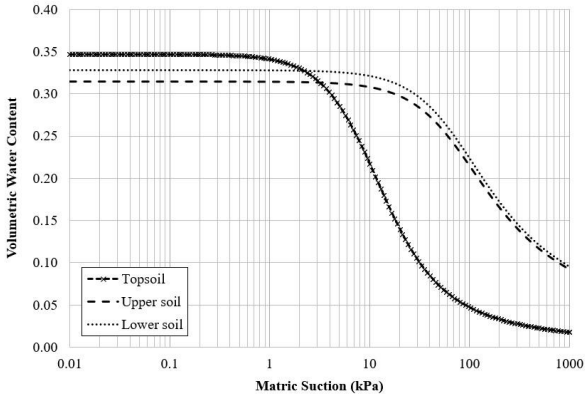

(a) SWCCs

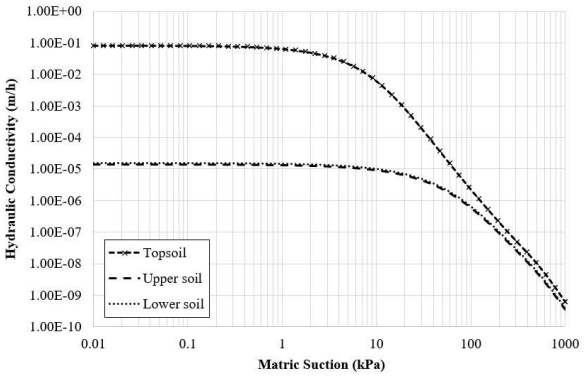

(b) HCFs

Figure 5. Soil water characteristic curves (SWCC) and hydraulic conductivity functions (HCF) used in seepage modeling

soil by measuring the propagation speed of an electromagnetic wave propagated through stainless steel rods. Five TDRs were installed in the test pit to measure the volumetric water content at various depths. The TDRs (TMC-04 model) used in this study were products of the National Electronics and Computer Technology Center of Thailand (NECTEC). Figure 2 shows locations of five TDRs (i.e., TDR 1 to TDR 5) installed in the test pit. With a data acquisition system connected wirelessly to a web server, the volumetric water

contents were monitored real time. More TDR details with its calibration and specification are described in Thumtuan *et al.* (2018) and Chalermyanont & Chup-uppakarn (2020).

5. Results and Discussion

The simulation results and field monitoring data are analyzed and presented in two sections. In the first section, the change of pore water pressure due to the infiltrating rainwater is demonstrated. Analysis of the increase in pore water pressure due to rainfall is performed in an attempt to examine how the rainwater infiltrates into high and low permeable soils. In the second section, verification of soil water content from the simulation results is made by comparing with the field monitoring data.

5.1 Transient seepage simulation results

Change of pore water pressure in response to infiltrating rainwater from the simulation results are shown in Figure 4. Before the rain, the soil is naturally unsaturated and having negative pore water pressure. After the rain, the seeping water turns the unsaturated soil to wet soil or saturated soil, while its pore water pressure increases and becomes zero or positive. For the topsoil (0.15 m), the pore water pressure promptly responds to rainfall as it increases or decreases according to the rain. For deeper soil layers (0.5-2.0 m) where the soils are less permeable, the pore water pressure slightly increases and does not respond much to the rain. For the upper layer, the soil at shallower depth (0.5 m) is more influenced by rainfall as reflected by the high increase of pore water pressure. In additions, during drying period (i.e., after November 6th), the soil starts to dry as its pore water pressure decreases till the end of the simulation.

Change of the pore water pressure with respect to depth and time in response to infiltrating rainwater are shown in Figure 6. Initially, the pore water pressure is very low (high negative value) near ground surface and increases linearly with depth as it is modelled using the initial groundwater table described previously. Subsequently, the pore water pressure increases with depth and time corresponding to the rainwater. The topsoil turns to be the saturated soil by October 20th, as its pore water pressure becomes positive. Positive pore water pressure at shallow depths is commonly observed after heavy rainfall in the monitored soil slopes (Gottlein & Mandercheid, 1988; Rezaur *et al.*, 2003). For deeper soils, the pore water pressure increases less than that of the topsoil due to less infiltrating rainwater. In the lower soil layer, very little water seeps down to this depth as little change in pore water pressure is observed. During the drying period, the pore water pressure of the shallow soils (0.15 and 0.5 m) starts decreasing as the water drains downslope. The topsoil becomes unsaturated soil again as its pore water pressure switches back to negative value.

Seepage of rainwater into the slope obtained from the transient seepage simulation up to November 4th is shown in Figure 7. At the middle of the slope where the test pit is located, the topsoil is mostly saturated, while negative pore water pressure is still evident in the deeper soils. The water seeps through the topsoil easily because it is high permeable silty sand. On the other hand, the other two soils which are much less permeable, thus, most of the water within the topsoil drains downslope to slope toe resulting in very little amount of water seeping into the upper and lower layers.

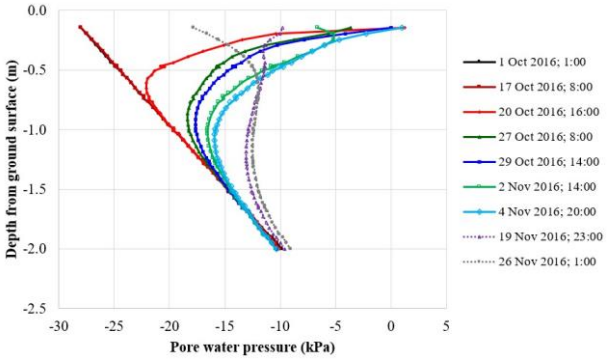

Figure 6. Simulated pore water pressure profiles at the test pit

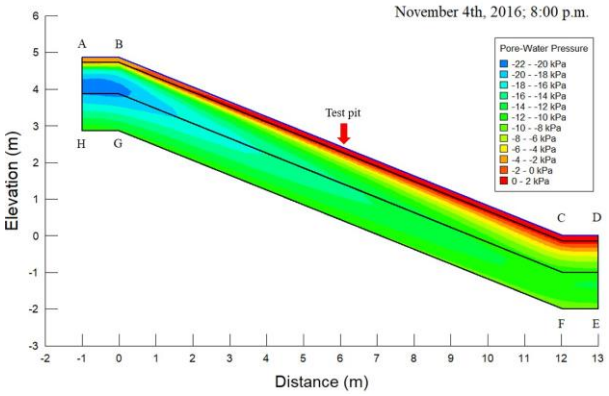

Figure 7. Simulated pore water pressure of the soil slope

5.2 Verification of the simulation results

Field monitoring data of soil volumetric water content measured using the TDRs as reported by Thumtuan *et al.* (2018) were compared to the simulation results. The simulated pore water pressure data discussed in previous sections were converted conveniently by SEEP/W to the volumetric water content and used for comparison. For ease of comparison and demonstration, the simulated and measured volumetric water contents for several days are shown in Figures 8. The simulated volumetric water contents compare fairly well to the measured ones as percent errors are less than 10% (i.e., 6.1 and 9.8% on average for wetting and drying period, respectively). It indicates that finite element modeling of transient seepage simulation can be used for estimating water content of the soil slope due to rainfall.

For shallow soils, the finite element model well predicts the volumetric water content as seen in Figures 8a-c. For example, on October 27th at 0.15 m depth, the simulated volumetric water content was 0.32 while the corresponding observed one was 0.30. However, for the lower soil (1.5–2.0 m), the simulation result seems to overestimate the volumetric water content. This is because of the fact that, the soil is naturally heterogeneous and anisotropic resulting in possible non-uniform distribution of water within the soil mass, thus, it can be drier (lower volumetric water content) than the

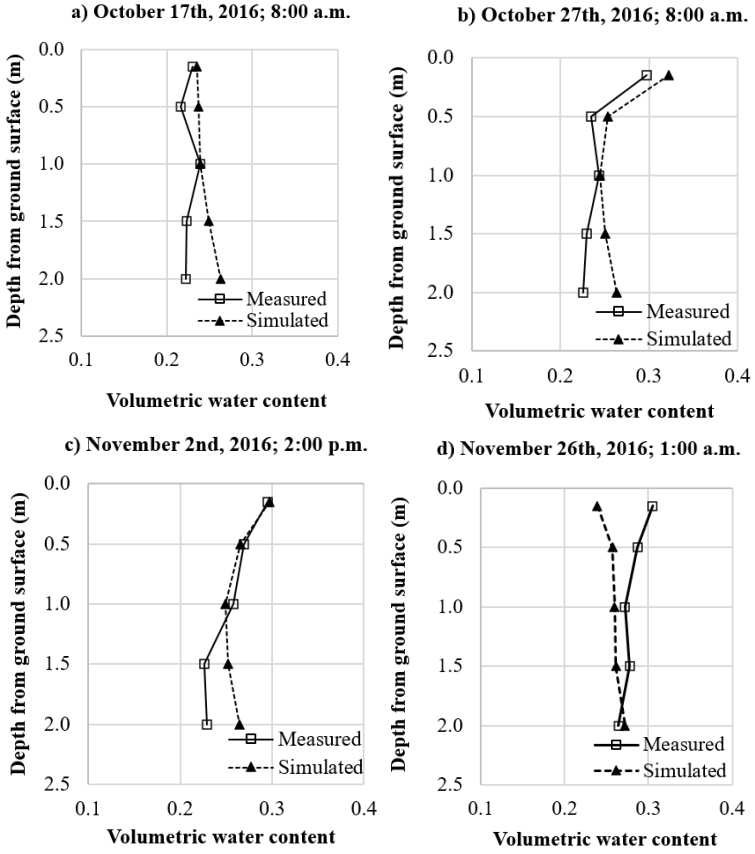

Figure 8. Comparison between simulated and measured volumetric water contents

simulated one where the pore water pressure is computed hydrostatically from the location of the groundwater table. A study of Winnipeg clay within a railway embankment by Sattler (1990) also reported the same results.

The soils start drying when the rainfall switched from wetting to drying period resulting in decreasing in the volumetric water content. The simulated volumetric water content, however, decreases more than that of the measured one (Figure 7d). The simulated results underestimate the volumetric water content as indicated by the percent error of 9.8%. Since there is hysteresis in the SWCC and HCF as reported by many researchers (Corey, 1977; Nielsen, Jackson, Cary, & Evans, 1972; Topp & Miller, 1966), thus, changes of the volumetric water content from wetting to drying and vice versa are different. The SEEP/W, however, does not incorporate the hysteresis function in the simulation which, in turns, may result in the underestimation of the volumetric water content in the drying period.

6. Conclusions

Transient seepage simulation was conducted on the residual soil slope using the finite element model to assess the change of soil water content due to rainfall. The residual soil samples were collected from a test pit and used to determine physical and hydrological properties required in the modeling. The soil slope consisted of three layers, namely; the topsoil, the upper and lower layers with total thickness of 2.2 m. The topsoil was permeable silty sand where the upper and lower layers were low permeable clayey gravel and high plasticity clay.

The simulation results showed that the topsoil solely responded to the rain as its pore water pressure promptly changed from negative to positive indicating that the infiltrating rainwater had changed the soil from unsaturated to saturated soil. For deeper soils, due to their low permeability, their pore water pressures slightly increased as the water in the topsoil marginally flow downward but mostly drained downslope to slope toe. To verify the simulation results, the soil volumetric water content data observed in the field using the TDRs were compared to the simulation results. The simulated volumetric water contents compared fairly well to the observed ones as percent errors were lower than 10 percent. Verification results indicated that the change of soil water content due to rainfall can be estimated by conducting the transient seepage modeling with availability of sufficient physical and hydrological properties of soils.

Acknowledgements

Authors gratefully acknowledge the financial support from Prince of Songkla University via Grant no. ENG580970S. The Department of Civil Engineering, and the Southern Natural Disaster Research Center, Faculty of Engineering, Prince of Songkla University are appreciated for their support.

References

Acharya, K. P., Bhandary, N. P., Dahal R. K., & Yatabe, R. (2016). Seepage and slope stability modelling of rainfall induced slope failures in topographic hollow. *Geomatics Natural Hazards and Risk, 7*(2), 721-746, doi:10.1080/19475705.2014.954150

Anderson, M. G., & Pope, R. G. (1984). The incorporation of soil water physics models into geotechnical studies of landslide behaviour. *Proceedings of the 4th, International Symposium on Landslides, 4*, 349-353.

Brunetti, M. T., Peruccacci, S., Rossi, M., Luciani, S., Valigi, D., & Guzzetti, F. (2010). Rainfall threshold for the possible occurrence of landslide in Italy. *Natural Hazards and Earth System Science, 10*, 447-458.

Chalermyanont, T., & Chub-Uppakarn, T. (2020). Seepage characteristic for stability evaluation of a residual soil slope: A case study of Khohong Mountain, Songkhla Province (ENG580970S). Hat Yai, Songkhla, Thailand: Faculty of Civil Engineering, Prince of Songkla University.

Corey, A. T. (1977). Mechanics of heterogeneous fluids and porous media. Fort Collins, CO: Water Resource Publication.

Department of Mineral Resources. (2007). Digital geological map of Songkhla Province, Thailand.

Electricity Generating Authority of Thailand. (1980). Soil exploration by Kunzelstab penetration test (in Thai).

Frattini, P., Crosta, G., & Sosio, R. (2009). Approaches for defining thresholds and return periods for rainfall-triggered shallow landslides. *Hydrological Process, 23*, 1444-1460.

Fredlund, D. G., & Rahardjo, H. (1993). *Soil mechanics for unsaturated soils*. New York, NY: John Wiley and Sons.

Fredlund, D. G., & Xing, A. (1994). Equations for the soil-water characteristic curve. *Can Geotech Journal, 31*(3), 521-523.

Gottlein, A., & Manderscheid, B. (1998). Spatial heterogeneity and temporal dynamics of soil water tension in a mature Norway spruce stand. *Hydrological Process, 12*(3), 417-428.

Iverson, R. M. (2000). Landslide triggering by rain infil tration. *Water Resource Research, 36*, 1897-1910.

Jiratananuwong, T., Chalermyanont, T., & Chub-Uppakarn. T. (2016). Analysis of a rainfall-triggered landslide and determination triggered landslide and determination of critical cumulative rainfall for landslide warning in southern thailand. *Geotechnics for Sustainable Infrastructure Development - Geotec Hanoi 2016*.

Leach, B., & Herbert, R. (1982). The genesis of numerical model for the study of the hydrology of a steep hillside in Hong Kong. Quarterly *Journal of Engineering. Geology, 15*, 243-259.

Lee, L. M., Gofar, N., & Rahardjo, H. (2009). A simple model for preliminary evaluation of rainfall induced slope stability. *Engineering Geology, 108*, 272-285.

Matshushi, Y., & Matsukura, Y. (2007). Rainfall thresholds for shallow landsliding derived from pressure-head monitoring: cases with permeable and impermeable bedrocks in Boso Peninsula, Japan. *Earth Surface Processes and Landforms, 32*, 1308-1322.

Montgomery, D. R., Dietrich, W. E., Torres, R., Anderson, S. P., Heffner, J. T., & Loague, K. (1997). Hydrologic response of a steep, unchanneled valley to natural and applied rainfall. *Water Resource Research, 33*, 91-109.

Nemes, A., Schaap, M. G., Leij, F. J. & Wösten, J. H. M. (2001). Description of the unsaturated soil hydraulic database UNSODA version 2.0. *Journal of Hydrology, 251*, 151–162.

Ng, C. W. W., & Shi, Q. (1998). A numerical investigation of the stability of unsaturated soil slope subjected to transient seepage. *Computers and Geotechnics, 22*(1), 1-28.

Nielsen, D. R., Jackson, R. D., Cary, J. W., & Evans, D. D. (1972). Soil water. Madison, WI: American Society of Agronomy and Soil Science.

Quinones, H., Ruelle, P., & Nemeth, I. (2003). Comparison of three calibration procedures for TDR soil moisture sensors. *Irrigation and Drain, 52*, 203–217.

Rahardjo, H., Leong, E. C., & Rezaur, R. B. (2002). Studies of rainfall-induced slope failures. *Proceeding of the National Seminar Slope 2002*, April 27, 2002, Bandung, Indonesia, 15–29.

Rahardjo, H., Ong, T. H., Rezaur, R. B., & Leong, E. C. (2007). Factors controlling instability of homo geneous soil slopes under rainfall. *Journal of Geotech and Geoenvironmental Engineering ASCE, 133*, 1532-1543.

Rahimi, A., Rahardjo, H., & Leong, E. C. (2010). Effect of hydraulic properties of soil on rainfall induced slope failure. *Journal of Engineering Geology, 114*, 135-143.

Rezaur1, R. B., Rahardjo, H., Leong, E. C., & Lee, T. T. (2003). Hydrologic behavior of residual soil slopes in Singapore. *Journal of Hydrologic Engineering*, May 2003.

Sattler, P. J. (1990). *Numerical modelling of vertical ground movement* (Master's thesis, University of Saskatchewan, Saskatoon, Canada).

Thumtuan, P., Chup-Uppakarn, T., & Chalermyanont, T. (2018). Real time monitoring of soil moisture content for landslide early warning: wn experimental study. *Proceedings of the MATEC Web Conferences 192, 02032 (2018), ICEAST 2018.* doi:10.1051/matecconf /201819202032.

Topp, G. C., Davis, J. L., & Annan, A. P. (1980). Electromagnetic determination of soil water content: measurements in coaxial transmission lines. *Water Resources Research, 16*, 574–582.

Topp, G. C., & Miller, E. E. (1966). Hysteretic moisture characteristics and hydraulics conductivities for glass-bead media. *Proceedings of Soil Science America, 30*, 156-162.

Uchida, T., Asano, Y., Ohte, N., & Mizuyama, T. (2003). Analysis of flow path dynamics in a steep unchannelled hollow in the Tanakami mountains of Japan. *Hydrological Processes, 17*, 417-430.

Wolle, C. M., & Hachich, W. (1989). Rain-induced landslides in south-eastern Brazil. *Proceedings of the 12th International Conference of Soil Mechanic and Foundation Engineering*, Rio de Janeiro, 3, 1639-1644.